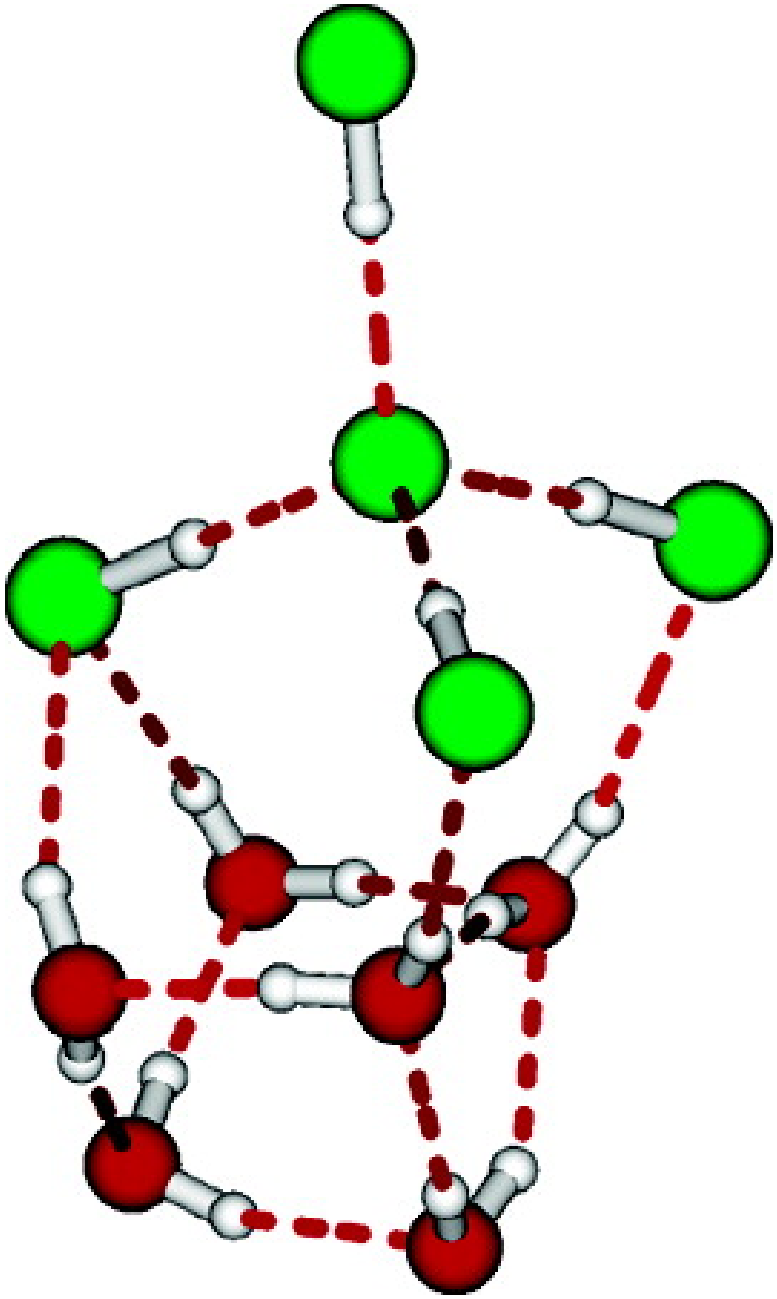

More About This Article

Additional resources and features associated with this article are available within the HTML version:

J|A|C|S
ARTICLES
Published on Web 02/23/2007

Reactions of Large Water Cluster Anions with Hydrogen Chloride: Formation of Atomic Hydrogen and Phase Separation in the Gas Phase

Chi-Kit Siu,[†,‡] O. Petru Balaj,[†,§] Vladimir E. Bondybey,[†] and Martin K. Beyer*[,†,||]

Contribution from the Department Chemie, Physikalische Chemie 2, Technische Universität München, Lichtenbergstrasse 4, 85747 Garching, Germany.

Received October 13, 2006; E-mail: martin.beyer@mail.chem.tu-berlin.de

Abstract: The reactions of water cluster anions $(H_2O)_n^-$, $n = 30-70$, with hydrogen chloride have been studied by Fourier transform ion cyclotron resonance (FT−ICR) mass spectrometry. The first HCl taken up by the clusters is presumably ionically dissolved. The solvated electron recombines with the proton, which is thereby reduced to atomic hydrogen and evaporates from the cluster. This process is accompanied by blackbody radiation and collision induced loss of water molecules. Subsequent collisions lead to uptake of HCl and loss of H_2O, yielding mixed clusters $Cl^-(HCl)_m(H_2O)_n$ until they are saturated with HCl. Those saturated clusters lose H_2O and HCl in a characteristic sequence. The final stage of the reaction, involving clusters with $m = 0-4$ and $n = 0-6$, is studied in detail with density functional theory calculations. The $Cl^-(HCl)_4(H_2O)_6$ cluster represents an example for supramolecular self-organization in the gas phase: it consists of a tetrahedral $Cl^-(HCl)_4$, connected on one side of the tetrahedron to a compact water hexamer.

Introduction

Solvated electrons have already been observed in the very early days of chemistry, almost 200 years ago. It took, however, almost a century of research, among others by Weyl,[1] before the early observation by Humphrey Davy of a deep blue color appearing when liquefied NH_3 came in contact with sodium or potassium was correctly interpreted by Kraus as being due to electrons solvated by the ammonia.[2]

The fact that solvated electrons can also be generated, at least transiently, in water is a much more recent discovery. They can be produced by a variety of methods, and their properties have become the main subject of what is called radiation chemistry.[3−5] In one type of such experiments, pulsed radiolysis, the liquid samples, mostly aqueous solutions, are irradiated by intense pulses of energetic electrons, with energies of several MeV. Another, more recently introduced alternative is to generate the electrons by multiphoton ionization using short, intense fs laser pulses.[6] These methods allow investigations of the dynamics of electron solvation and kinetics of their chemical reactions by monitoring the appearance of their spectrum and of its subsequent decay, as well as the appearance of their reaction products in a variety of pump−probe experiments.[7,8]

Such reactions of electrons in solution are not only of purely academic interest, but also, in fact, of considerable practical, technical, and industrial importance. For example, one important field of application lies in the purification of water. The extensive use of polychlorinated biphenyls, chlorinated aliphatic hydrocarbons, and other halogenated compounds represents a major environmental problem, since many are highly toxic, and they often have a very long lifetime in the environment. Many of these species can be very efficiently dechlorinated by means of radiolysis, followed by reactions involving hydrated electrons.[9−11]

In recent decades, it was demonstrated that besides bulk solutions, electrons solvated in small, finite clusters[12−14] can also be prepared in experiments with cold, supersonic beams. Their spectroscopy and dynamics have been studied in detail,[15−19]

† Technische Universität München.
‡ Current address: Department of Chemistry and Centre for Research in Mass Spectrometry, York University, 4700 Keele Street, Toronto, Ontario, Canada M3J1P3.
§ Current address: Ecole Polytechnique, Departement de Chimie, UMR 7651, Laboratoire DCMR, Route de Saclay, 91128 Palaiseau CEDEX, France.
|| Current address: Institut für Chemie, Sekr. C4, Technische Universität Berlin, Strasse des 17. Juni 135, 10623 Berlin, Germany.

(1) Weyl, W. *Ann. Phys. (Weinheim, Ger.)* **1864**, *121*, 601−612.
(2) Kraus, C. A. *J. Am. Chem. Soc.* **1908**, *30*, 1323.
(3) Anbar, M. *Adv. Phys. Org. Chem.* **1969**, *7*, 115.
(4) Schindewolf, U. *Angew. Chem., Int. Ed. Engl.* **1968**, *7*, 190.
(5) Buxton, G. V.; Greenstock, C. L.; Helman, W. P.; Ross, A. B. *J. Phys. Chem. Ref. Data* **1988**, *17*, 513−886.
(6) Kimura, Y.; Alfano, J. C.; Walhout, P. K.; Barbara, P. F. *J. Phys. Chem.* **1994**, *98*, 3450−3458.
(7) Laenen, R.; Roth, T.; Laubereau, A. *Phys. Rev. Lett.* **2000**, *85*, 50−53.
(8) Son, D. H.; Kambhampati, P.; Kee, T. W.; Barbara, P. F. *J. Phys. Chem. A* **2001**, *105*, 8269−8272.
(9) Singh, A.; Kremers, W. *Radiat. Phys. Chem.* **2002**, *65*, 467−472.
(10) Chaychian, M.; Silverman, J.; Al-Sheikhly, M.; Poster, D. L.; Neta, P. *Environ. Sci. Technol.* **1999**, *33*, 2461−2464.
(11) Schmelling, D. C.; Poster, D. L.; Chaychian, M.; Neta, P.; Silverman, J.; Al-Sheikhly, M. *Environ. Sci. Technol.* **1998**, *32*, 270−275.
(12) Haberland, H.; Ludewigt, C.; Schindler, H. G.; Worsnop, D. R. *J. Chem. Phys.* **1984**, *81*, 3742−3744.
(13) Haberland, H.; Langosch, H.; Schindler, H. G.; Worsnop, D. R. *J. Phys. Chem.* **1984**, *88*, 3903−3904.
(14) Haberland, H.; Schindler, H. G.; Worsnop, D. R. *Ber. Bunsen-Ges. Phys. Chem.* **1984**, *88*, 270−272.
(15) Ayotte, P.; Johnson, M. A. *J. Chem. Phys.* **1997**, *106*, 811−814.
(16) Hammer, N. I.; Shin, J. W.; Headrick, J. M.; Diken, E. G.; Roscioli, J. R.; Weddle, G. H.; Johnson, M. A. *Science* **2004**, *306*, 675−679.

10.1021/ja067355o CCC: $37.00

starting with the photoelectron spectroscopy work by Bowen and co-workers.[20] Also available is a large number of sophisticated theoretical investigations.[21−23]

We have been using a very efficient laser vaporization source[24−27] to produce and study a variety of hydrated ions.[28−32] Employing Fourier transform ion cyclotron resonance (FT−ICR) mass spectrometry, we were able to store and mass select the hydrated electron clusters, $(H_2O)_n^-$, and investigate their stability and the competition between their gradual fragmentation and the electron detachment induced by the absorption of infrared blackbody radiation.[33] Such finite clusters can, however, also be a very convenient medium for the studies of chemical reactions. Since the FT−ICR measurements yield unambiguous information about the elemental composition of the clusters, the effects of impurities which always plague experiments in bulk solutions can be completely eliminated. Reactions with acetonitrile, carbon dioxide, oxygen, and other species revealed a number of interesting properties of the chemistry of the hydrated electron,[34−37] building on the pioneering flow-tube experiments by Johnson, Viggiano, and co-workers.[38,39] In the present manuscript, we examine the behavior of the hydrated electron clusters in the presence of hydrogen chloride as reagent.

Recombination of a solvated electron with a proton may be viewed as the simplest and most fundamental electrochemical reaction. In bulk solution, however, it proved difficult to follow this reaction directly. Hardly anybody will doubt that this reaction actually takes place in solution, and it is routinely described in radiation chemistry literature as the primary decay pathway of the hydrated electron, unless strongly basic buffers are used.[40,41] Yet, the first reports on its observation sparked a heated debate.[42−45] The goal of our recent research is to use reactions of water cluster anions as models for solution phase solvated electrons.[36] Using formic acid as a reactant,[37] hydrogen elimination was observed only with a branching ratio of 10%, while, in 90% of the cases, the electron was solvated and stabilized by formic acid molecules. A thermochemical analysis showed that hydrogen elimination is endothermic in this case. However, formic acid is not strongly dissociated in aqueous solution, and this motivated us to reinvestigate this reaction with HCl. While our experiments, in which the proton is introduced into the water cluster anion by ionic dissolution of HCl, unambiguously show that the fundamental recombination of the proton with the electron really occurs in the cluster, the secondary reactions proved to be even more exciting. The major part of this manuscript therefore describes the reactions of $Cl^-(H_2O)_n$, which are formed as primary reaction products, with further molecules of HCl.

Experimental Details

The experiments were performed using a 4.7 T Bruker/Spectrospin CMS47X FT−ICR mass spectrometer equipped with an APEX III Data Station, a Bruker infinity cell, and a home-built laser vaporization source described in detail previously.[25,28,33,34] Hydrated electrons were generated by laser vaporization of a rotating metal target, followed by supersonic expansion of the hot plasma in a 50 μs gas pulse of helium seeded with water vapor.[28,33,34] The charged clusters are accelerated, guided by electrostatic lenses, transferred through four stages of differential pumping, decelerated, and finally trapped in the ICR cell at a background pressure of 2×10^{-10} mbar. In the present investigation we have used a target made from pressed Zn powder (Aldrich, 99.9%+). Due to the negative electron affinity of Zn, the formation of $Zn_n(H_2O)_n^-$ is avoided, which results in an intense, clean distribution of hydrated electrons $(H_2O)_n^-$, essentially free of other anionic species.[33−36]

The reactant gas hydrogen chloride (Aldrich, 99+%) is introduced into the ultrahigh vacuum region through a needle valve, adjusted to raise the pressure in the analysis cell to the desired value, typically 6.0×10^{-9} mbar. The mass spectra of the species accumulated in the ICR cell are taken at the end of the trapping cycle, and then after various reaction delays, in order to monitor the progress of the reaction, decay of the pure electron clusters, and the formation of products. The vacuum chamber enclosing the ICR cell was kept at a constant temperature of 290 ± 6 K by water flowing through a cooling jacket.

Computational Details

We have employed the Becke three-parameter hybrid functional and the Lee−Yang−Parr correlation functional (B3LYP) together with the 6-311++G** basis set, implemented in the Gaussian03 program,[46] to optimize the geometry and compute the harmonic frequencies of clusters $Cl^-(HCl)_n(H_2O)_m$.

The Vienna Ab Initio Simulation Package[47−50] was used to find low lying isomers of $Cl^-(HCl)_4(H_2O)_6$. The details of the molecular dynamics simulations are similar to that in our recent work.[51] Briefly,

(17) Bragg, A. E.; Verlet, J. R. R.; Kammrath, A.; Cheshnovsky, O.; Neumark, D. M. *Science* **2004**, *306*, 669−671.
(18) Paik, D. H.; Lee, I. R.; Yang, D. S.; Baskin, J. S.; Zewail, A. H. *Science* **2004**, *306*, 672−675.
(19) Verlet, J. R. R.; Bragg, A. E.; Kammrath, A.; Cheshnovsky, O.; Neumark, D. M. *Science* **2005**, *307*, 93−96.
(20) Coe, J. V.; Lee, G. H.; Eaton, J. G.; Arnold, S. T.; Sarkas, H. W.; Bowen, K. H.; Ludewigt, C.; Haberland, H.; Worsnop, D. R. *J. Chem. Phys.* **1990**, *92*, 3980−3982.
(21) Barnett, R. N.; Landman, U.; Dhar, S.; Kestner, N. R.; Jortner, J.; Nitzan, A. *J. Chem. Phys.* **1989**, *91*, 7797−7808.
(22) Kim, J.; Becker, I.; Cheshnovsky, O.; Johnson, M. A. *Chem. Phys. Lett.* **1998**, *297*, 90−96.
(23) Jordan, K. D. *Science* **2004**, *306*, 618−619.
(24) Bondybey, V. E.; English, J. H. *J. Chem. Phys.* **1981**, *74*, 6978−6979.
(25) Berg, C.; Schindler, T.; Niedner-Schatteburg, G.; Bondybey, V. E. *J. Chem. Phys.* **1995**, *102*, 4870−4884.
(26) Dietz, T. G.; Duncan, M. A.; Powers, D. E.; Smalley, R. E. *J. Chem. Phys.* **1981**, *74*, 6511−6512.
(27) Maruyama, S.; Anderson, L. R.; Smalley, R. E. *Rev. Sci. Instrum.* **1990**, *61*, 3686−3693.
(28) Beyer, M.; Berg, C.; Görlitzer, H. W.; Schindler, T.; Achatz, U.; Albert, G.; Niedner-Schatteburg, G.; Bondybey, V. E. *J. Am. Chem. Soc.* **1996**, *118*, 7386−7389.
(29) Niedner-Schatteburg, G.; Bondybey, V. E. *Chem. Rev.* **2000**, *100*, 4059−4086.
(30) Bondybey, V. E.; Beyer, M. K. *Int. Rev. Phys. Chem.* **2002**, *21*, 277−306.
(31) Fox, B. S.; Balaj, O. P.; Balteanu, L.; Beyer, M. K.; Bondybey, V. E. *Chem.—Eur. J.* **2002**, *8*, 5534−5540.
(32) Fox, B. S.; Beyer, M. K.; Bondybey, V. E. *J. Am. Chem. Soc.* **2002**, *124*, 13613−13623.
(33) Beyer, M. K.; Fox, B. S.; Reinhard, B. M.; Bondybey, V. E. *J. Chem. Phys.* **2001**, *115*, 9288−9297.
(34) Balaj, O. P.; Balteanu, I.; Fox-Beyer, B. S.; Beyer, M. K.; Bondybey, V. E. *Angew. Chem., Int. Ed.* **2003**, *42*, 5516−5518.
(35) Balaj, O. P.; Siu, C. K.; Balteanu, I.; Beyer, M. K.; Bondybey, V. E. *Chem.—Eur. J.* **2004**, *10*, 4822−4830.
(36) Balaj, O. P.; Siu, C. K.; Balteanu, L.; Beyer, M. K.; Bondybey, V. E. *Int. J. Mass Spectrom.* **2004**, *238*, 65−74.
(37) Reitmeier, S. J.; Balaj, O. P.; Bondybey, V. E.; Beyer, M. K. *Int. J. Mass Spectrom.* **2006**, *249*, 106−111.
(38) Posey, L. A.; Deluca, M. J.; Campagnola, P. J.; Johnson, M. A. *J. Phys. Chem.* **1989**, *93*, 1178−1181.
(39) Arnold, S. T.; Morris, R. A.; Viggiano, A. A.; Johnson, M. A. *J. Phys. Chem.* **1996**, *100*, 2900−2906.
(40) Schwarz, H. A. *J. Phys. Chem.* **1992**, *96*, 8937−8941.
(41) Buxton, G. V.; Mulazzani, Q. G.; Ross, A. B. *J. Phys. Chem. Ref. Data* **1995**, *24*, 1055−1349.
(42) Kongshaug, M.; Steen, H. B.; Cercek, B. *Nat. Phys. Sci.* **1971**, *234*, 97.
(43) Nielsen, S. O. *Nat. Phys. Sci.* **1972**, *240*, 21−22.
(44) Neta, P.; Schuler, R. H.; Fessenden, R. W. *Nat. Phys. Sci.* **1972**, *237*, 46−47.
(45) Kongshaug, M.; Steen, H. B.; Cercek, B. *Nat. Phys. Sci.* **1972**, *237*, 47.
(46) Frisch, M. J., et al. *Gaussian 03*, revision B.01; Gaussian, Inc.: Pittsburgh, PA, 2003.
(47) Kresse, G.; Furthmuller, J. *Phys. Rev. B* **1996**, *54*, 11169−11186.
(48) Kresse, G.; Furthmuller, J. *Comput. Mater. Sci.* **1996**, *6*, 15−50.
(49) Kresse, G.; Hafner, J. *Phys. Rev. B* **1994**, *49*, 14251−14269.
(50) Kresse, G.; Hafner, J. *Phys. Rev. B* **1993**, *47*, 558−561.

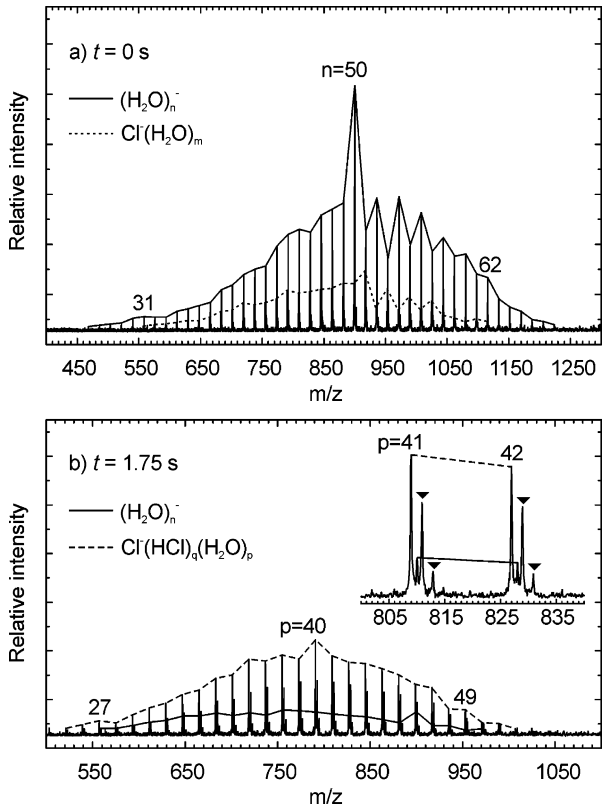

Figure 1. Mass spectra of the reaction of $(H_2O)_n^-$ with HCl. (a) At nominal $t = 0$ s, the clusters have been accumulated during 2 s in the ICR cell, and some of them have already reacted by elimination of an H atom and formation of $Cl^-(H_2O)_m$. (b) After an additional $t = 1.75$ s, most of the clusters have already taken up a second HCl molecule, as evidenced by the isotope pattern of $Cl^-(HCl)_q(H_2O)_p$ (▼), where $q = 1,2$.

the density functional theory with the Perdew−Wang gradient correction was used. The pseudopotentials for the core elctrons of the atoms were constructed by the projector augmented wave (PAW) method. The electronic wavefunction was described by a planewave basis set with a cutoff energy of 280 eV. The molecular dynamics of the ion in a cubic box with a dimension of 18 Å was simulated with an integration time step of 0.5 fs.

Results and Discussion

FT−ICR Mass Spectrometric Studies of Reactions of $(H_2O)_n^-$ with HCl. Our cluster source yields $(H_2O)_n^-$ water cluster anions with n values extending from about 15 to nearly 100. As we have previously shown, the low end limit is due to rapid electron detachment from small clusters, while at the upper end the distribution is limited by the increasing rates of room-temperature blackbody radiation induced fragmentation.[33] The range in a specific experiment depends on the conditions of the laser vaporization source and the time-of-flight parameters between the source and the cell, with a typical distribution in one of our experiments being exemplified in Figure 1a, where the clusters extend over the range $n = 30-70$.

Figure 1a shows the measured distribution at a nominal time $t = 0$ s. The clusters produced in the pulsed supersonic expansion are accumulated over 20 pulses or 2 s. Since HCl is present in the cell at a constant pressure, the reaction proceeds during the accumulation, and some products of the composition $Cl^-(H_2O)_n$ are therefore detected already at nominally $t = 0$ s. The interpretation of the spectra is made difficult by the fact that the mass of $H^{35}Cl$ is equal to that of 2 H_2O. The resolution of ICR mass spectrometry is in principle sufficient to resolve the small mass difference of 0.05 u, but in the presence of a reaction gas, it is significantly reduced, so that the lines of an $(H_2O)_n^-$ solvated electron would not be clearly separated from that of an $(HCl)(H_2O)_{n-2}^-$ at the same nominal mass. The ^{37}Cl isotope, however, with a natural abundance of 25%, allows unambiguous identification of the reaction products. The mass spectrum after 1.75 s in Figure 1b suggests that the primary reaction step is the uptake of HCl, with, on the time scale of the ICR instrument, immediate elimination of an H atom. Due to the overlap with $H_2{}^{18}O$, a minor contribution of very short-lived $(HCl)(H_2O)_n^-$ as a primary reaction product, which quickly releases hydrogen to form $Cl^-(H_2O)_n$, cannot be rigorously ruled out but seems unlikely.

Figure 2 shows an experiment where the $(H_2O)_{35}^-$ cluster at a nominal mass of 630 u was mass selected. $X^{\pm}(H_2O)_n$ hydrated ion clusters fragment due to absorption of room-temperature blackbody radiation.[52−59] The rates of this fragmentation are to a fair approximation independent of the specific nature of the central species X but are roughly proportional to the number of ligands n.[54,55,60] In the range around $n = 35$ the fragmentation rate is around 7 s^{-1}, and this makes it experimentally difficult to mass select a single peak. Due to this process, there are already some 15% $(H_2O)_{34}^-$ at mass 612 u present in Figure 2a, at a nominal time $t = 0$ s.

In Figure 2b, corresponding to a 0.1 s reaction time, one observes a considerable growth of the $n = 34$ fragmentation product at 612 u, with two additional peaks appearing, a stronger one at 611 u and one barely visible at 613 u. If the HCl was simply dissolved in the cluster, with three water ligands being vaporized by the heat of the reaction, then a peak due to clusters containing $H^{35}Cl$ should be at a nominal mass of 612 u, identical to that of the $n = 34$ fragmentation product. The corresponding peak due to $H^{37}Cl$, however, is expected at 614 u, but none is observed, and the $H_2{}^{18}O$ component of the reactant ions was resonantly ejected. Absolute mass measurements are consistent with the assignment that the 611 u and 613 u product species correspond to clusters with an elemental composition of $^{35}Cl^-(H_2O)_{32}$ and $^{37}Cl^-(H_2O)_{32}$, respectively. Since the $(H_2O)_{35}^-$ reactant must be responsible for the growth of these products, the following reactions are apparently taking place:

$$(H_2O)_{35}^- + h\nu \rightarrow (H_2O)_{34}^- + H_2O \quad (1)$$

$$(H_2O)_{35}^- + HCl \rightarrow Cl^-(H_2O)_{32} + H + 3\,H_2O \quad (2)$$

(51) Siu, C.-K.; Fox-Beyer, B. S.; Beyer, M. K.; Bondybey, V. E. *Chem.—Eur. J.* **2006**, *12*, 6382−6392.
(52) Dunbar, R. C. *J. Phys. Chem.* **1994**, *98*, 8705−8712.
(53) Dunbar, R. C.; McMahon, T. B. *Science* **1998**, *279*, 194−197.
(54) Fox, B. S.; Beyer, M. K.; Bondybey, V. E. *J. Phys. Chem. A* **2001**, *105*, 6386−6392.
(55) Schindler, T.; Berg, C.; Niedner-Schatteburg, G.; Bondybey, V. E. *Chem. Phys. Lett.* **1996**, *250*, 301−308.
(56) Schnier, P. D.; Price, W. D.; Jockusch, R. A.; Williams, E. R. *J. Am. Chem. Soc.* **1996**, *118*, 7178−7189.
(57) Sena, M.; Riveros, J. M. *Rapid Commun. Mass Spectrom.* **1994**, *8*, 1031−1034.
(58) Thölmann, D.; Tonner, D. S.; McMahon, T. B. *J. Phys. Chem.* **1994**, *98*, 2002−2004.
(59) Weis, P.; Hampe, O.; Gilb, S.; Kappes, M. M. *Chem. Phys. Lett.* **2000**, *321*, 426−432.
(60) Fox, B. S.; Balteanu, I.; Balaj, O. P.; Liu, H. C.; Beyer, M. K.; Bondybey, V. E. *Phys. Chem. Chem. Phys.* **2002**, *4*, 2224−2228.

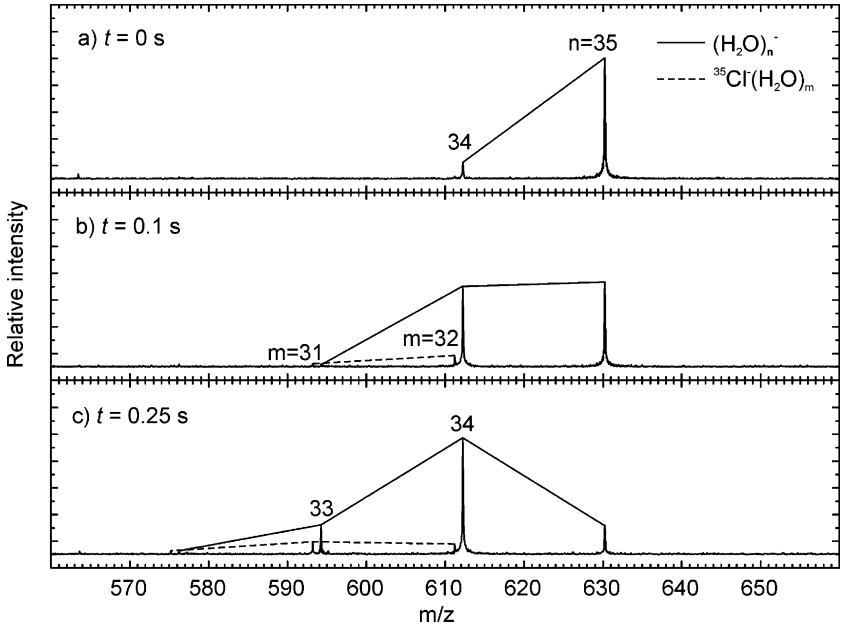

Figure 2. Mass spectra of the reaction of size-selected $(H_2O)_{35}^-$ with HCl after a (a) 0 s, (b) 0.1 s, and (c) 0.25 s reaction delay. The main fraction of the clusters fragment due to heating by blackbody radiation to form $(H_2O)_{34}^-$, while some collide with HCl and form $Cl^-(H_2O)_{32}$.

Here reaction 1 corresponds to the blackbody radiation induced dissociation. In reaction 2, the hydrogen chloride molecule is taken up by the hydrated electron clusters, and besides evaporation of most likely three water ligands, also a hydrogen atom is lost, but the present data do not give information about the exact sequence of events involved in reaction 2. We know from our previous studies of other ionic water clusters that hydrogen chloride is ionically dissolved in the clusters.[30,31,61−65] It is natural to assume that also, in the present case, the dissolution and ionization of HCl in the large hydration shell, giving rise to aqueous H^+ and Cl^- ions, is the first reaction step. Subsequently the electron would recombine with the proton, yielding a neutral hydrogen atom which interacts only weakly with the water solvation shell and evaporates from the cluster on a time scale which cannot be resolved in the ICR, i.e., faster than 1 ms. An alternative course of the reaction would be a rapid and direct transfer of the electron to the hydrogen chloride prior to its dissociation on the cluster surface, yielding HCl^-. This unstable anion would then nearly instantly dissociate to yield a chloride anion and a hydrogen atom, which would again evaporate from the surface.

Apparently the entire reaction, i.e., the dissolution of hydrogen chloride followed by the reduction of the hydrogen ion, is sufficiently exothermic to evaporate three molecules of water from the cluster, together with a thermochemically unfavorable hydrogen atom. Unfortunately, the number of evaporating water molecules could not be obtained more accurately, since the overlap of the reactant and product species together with theunfavorable isotope pattern of chlorine did not allow the quantitative analysis which was performed in the case of formic acid,[37] so a number with an uncertainty of 3.0 ± 0.5 evaporating water molecules is assumed. Evaporation of a water molecule is equivalent to a reaction enthalpy of $\sim 38 \pm 2$ kJ/mol,[37,39,66] which amounts to an enthalpy of ΔH(reaction 2) $= -114 \pm 19$ kJ/mol for the equivalent reaction for the charged species in a finite hydration environment. Literature thermochemistry allows the calculation of the enthalpy of the corresponding reaction in bulk solution:

$HCl(g)$	$\rightarrow H(g) + Cl(g)$	$\Delta H = +431.96$ kJ/mol[67]	(3)
$Cl(g) + e^-(g)$	$\rightarrow Cl^-(g)$	$\Delta H = -354.81$ kJ/mol[67]	(4)
$Cl^-(g)$	$\rightarrow Cl^-(aq)$	$\Delta H = -364$ kJ/mol[67]	(5)
$e^-(aq)$	$\rightarrow e^-(g)$	$\Delta H = +171.9 \pm 3.8$ kJ/mol[68]	(6)
$HCl(g) + e^-(aq)$	$\rightarrow Cl^-(aq) + H(g)$	$\Delta H = -115 \pm 4$ kJ/mol	(7)

The enthalpies of reaction 5 and 6 relate to a hydration enthalpy of the proton of −1090 kJ/mol, which is currently under debate. However, in the overall calculation this value cancels out, so that the error given for the enthalpy of reaction 7 is not affected. The number of evaporated water molecules in reaction 2 reflects the thermochemistry of the reaction, illustrated by the accidentally excellent numerical agreement. This suggests that "cluster phase" experiments indeed offer a direct route to condensed phase thermochemistry by counting the number of evaporating water molecules, as outlined previously by Arnold et al.,[39] complementary to the more elaborate scheme put forward by Coe.[69]

(61) Schindler, T.; Berg, C.; Niedner-Schatteburg, G.; Bondybey, V. E. *Chem. Phys. Lett.* **1994**, *229*, 57−64.
(62) Berg, C.; Beyer, M.; Achatz, U.; Joos, S.; Niedner-Schatteburg, G.; Bondybey, V. E. *Chem. Phys.* **1998**, *239*, 379−392.
(63) Beyer, M.; Achatz, U.; Berg, C.; Joos, S.; Niedner-Schatteburg, G.; Bondybey, V. E. *J. Phys. Chem. A* **1999**, *103*, 671−678.
(64) Fox, B. S.; Balaj, O. P.; Balteanu, I.; Beyer, M. K.; Bondybey, V. E. *J. Am. Chem. Soc.* **2002**, *124*, 172−173.
(65) Fox, B. S.; Beyer, M. K.; Achatz, U.; Joos, S.; Niedner-Schatteburg, G.; Bondybey, V. E. *J. Phys. Chem. A.* **2000**, *104*, 1147−1151.
(66) Shi, Z.; Ford, J. V.; Wei, S.; Castleman, A. W. *J. Chem. Phys.* **1993**, *99*, 8009−8015.
(67) Atkins, P. W. *Physikalische Chemie*; VCH: Weinheim, 1990.
(68) Shiraishi, H.; Sunaryo, G. R.; Ishigure, K. *J. Phys. Chem.* **1994**, *98*, 5164−5173.
(69) Coe, J. V. *Int. Rev. Phys. Chem.* **2001**, *20*, 33−58.

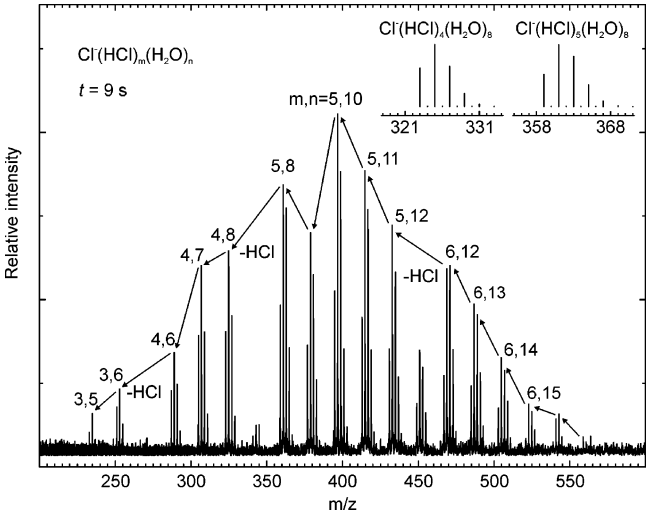

Figure 3. Mass spectrum of the reaction of $(H_2O)_n^-$, $n = 28-57$, with HCl after a reaction delay of 9 s. The clusters are almost completely saturated with HCl. Collisionally and blackbody radiation induced dissociation lead to evaporation of H_2O or HCl, depending on the cluster size. HCl loss preferentially occurs at $n = 6$, 8, and 12 H_2O molecules. The inset in the top right corner shows isotope patterns calculated from the natural abundance of ^{35}Cl and ^{37}Cl, which together with absolute mass measurements confirm the peak assignment.

Over the entire range of n values, we did not observe any products of the composition $(HCl)(H_2O)_n^-$, that is, clusters where the HCl was dissolved, without loss of a hydrogen atom. This is in contrast to our earlier experiment with formic acid, where only 15% of the reactions lead to hydrogen formation. This is most likely due to the less favorable thermochemistry; only one water molecule evaporates in the equivalent of reaction 2.[37] Obviously, the intracluster charge-transfer processes, the reduction of the proton, and elimination of atomic hydrogen must be very fast compared with the time scale of the experiment. The reaction products observed in Figure 2b can react and fragment further, as can be seen in panel 2c, corresponding to a reaction time of 0.25 s. Here only about 25% of the $(H_2O)_{35}^-$ reactant is left, while $(H_2O)_{34}^-$ is now by far the strongest peak, and its consecutive fragmentation products $n = 33$ and $n = 32$ can be seen. Also seen, although weak, are the $^{37}Cl^-(H_2O)_{32}$ redox reaction product and analogous clusters with 31 and even 30 water ligands.

The primary products $Cl^-(H_2O)_n$ collide with additional HCl molecules, and further reactions take place. Examination of products at longer times reveals that the water clusters can take up additional HCl molecules, but such subsequent steps are conceptually different from the first one. Even though the additional HCl molecules might again dissociate ionically to form the H^+ and Cl^- ions, the cluster now no longer contains a free electron, so that no reduction of the proton can take place.

As the reaction is allowed to run further, the uptake of HCl proceeds concurrently with cluster fragmentation, and the overall distribution of the clusters continuously shifts to smaller sizes and smaller values of n. One finds, however, that after a certain time only the fragmentation takes place, with the clusters no longer being able to take up additional HCl molecules. Such a situation is exemplified in Figure 3, which shows the products after a 9 s reaction delay. Each of the original, single peaks corresponding to the specific $(H_2O)_n^-$ clusters is replaced by a multiplet of several lines. As noted above, chlorine has two isotopes with natural abundances occurring in a ratio of about 3:1, and one can therefore from the pattern of each multiplet easily determine the number of chlorine atoms present in the product cluster. Thus, for a cluster containing a single chlorine, two lines in a ratio of 3:1 are expected, two chlorine atoms should give roughly a 9:6:1 triplet, three should give a 27:27:9:1 quartet, and so on. These isotopic multiplets then provide fingerprints from which the elemental composition of each cluster size can easily be inferred. Calculated exact isotope patterns are shown in the top right panel of Figure 3 for the clusters with five and six chlorine atoms.

The experiment started with a distribution of much larger $(H_2O)_n^-$ clusters, $n = 30-70$. Since the collisional rate is of the order of 1 s^{-1}, after 9 s, these clusters are essentially saturated with HCl. Subsequently, they only lose ligands, either due to the above-mentioned blackbody radiation or collisions. One should expect that, at each stage, the most weakly bound ligand is most likely to be lost.

If one now examines the spectra with this in mind, an interesting pattern emerges, with a cluster of a given number of water molecules containing a characteristic number of HCl molecules to form mixed clusters, $Cl^-(HCl)_m(H_2O)_n$, denoted by the indexes $[m,n]$ in the following discussion. At a reaction delay of 9 s, we observe compositions of $[m,n]$ with $m = 6$ and $n = 12-17$ for the largest clusters. For lighter ions, one finds $m = 5$ and with $n = 8-13$ remaining water molecules, $m = 4$ and $n = 6-8$ water ligands, and, finally, clusters with $m = 3$ and $n = 5-6$ water molecules. Interestingly, these ranges differing by the value of m, that is, by the number of HCl molecules, are clearly separated by gaps, where one cluster size or one of the chlorine multiplets seems to be missing or almost missing.

The order in which individual ligands are lost can be nicely followed in Figure 3. Starting, for instance, from an $[m,n] = [6,15]$ cluster, it will gradually lose water ligands, one by one. When the number of water molecules has dropped from $n = 15$ to $n = 12$ resulting in the [6,12] cluster, one of the HCl molecules is apparently more weakly bound than the remaining water ligands and will evaporate preferentially. This yields a [5,12] cluster and results in the loss of 36 u, leaving a gap or intensity minimum at a mass which would have corresponded to the loss of a single water ligand, 18 u. This gap corresponds to a [6,11] cluster, which is not observed. However, a small amount of [5,13] is observed in its place, which is probably due to large clusters which have only taken up 5 HCl, i.e., which are not yet fully saturated. In this way the fragmentation continues, with the cluster at each point shedding the most weakly bound ligand, either H_2O or HCl.

After a 20 s reaction delay, Figure 4a, the most intense peak groups in the spectrum correspond to the presence of only three and four chlorine atoms, such as $Cl^-(HCl)_2(H_2O)_{2-5}$ and $Cl^-(HCl)_3(H_2O)_{5,6}$. The fragmentation now slows down, since the remaining small clusters absorb blackbody radiation at a significantly reduced rate due to the reduced number of vibrational modes. At this point also ligand exchange becomes competitive with fragmentation. Since only HCl is present in the ICR cell, this can proceed only in one direction and results in a gradual exchange of the remaining H_2O with HCl.

The remaining ligands in the small clusters are all relatively strongly bound, and the nearly thermoneutral, or even slightly

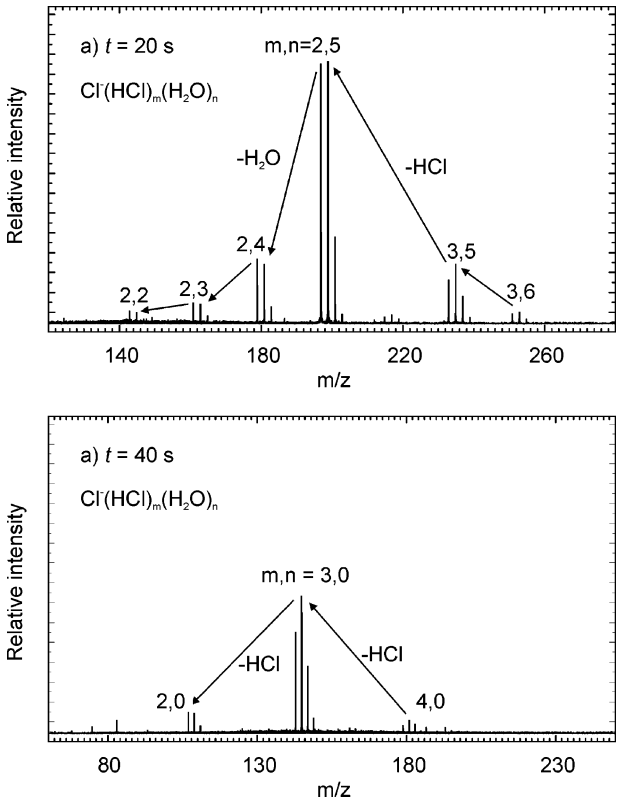

Figure 4. Mass spectra of the reaction of $(H_2O)_n^-$, $n = 28-57$, with HCl after (a) 20 s and (b) 40 s. The last time HCl is evaporated from a mixed cluster occurs from the [3,5] to the [2,5] species, as shown in spectrum a. The remaining [2,*n*] species undergo a slow ligand exchange, resulting in $Cl^-(HCl)_m$ or [*m*,0], $m = 2-4$, which further lose HCl until the final $m = 2$ cluster is reached, as indicated in spectrum b.

endothermic, ligand exchanges result ultimately in complete loss of water, so that after a 40 s reaction delay, the only observable mass peaks are due to the $Cl^-(HCl)_{2-4}$. The most intense group of five peaks corresponds to the $m = 3$, C_{3v} $Cl^-(HCl)_3$ complex ion, as can be seen in Figure 4b. In agreement with the theoretical computations, which will be discussed below, this ion cluster then only very reluctantly loses HCl, to form the $m = 2$, C_{2v} $Cl^-(HCl)_2$ cluster. Again consistent with the calculations, this cluster ion is too strongly bound to lose an additional HCl molecule.

Density Functional Theory Studies of $Cl^-(HCl)_m(H_2O)_n$. To assist in the interpretation of the last reaction stage, we have carried out a series of density functional theory (DFT) computations on the structure of mixed $Cl^-(HCl)_m(H_2O)_n$ clusters $[m,n] = [1-4,0-6]$. The "pure" clusters, $Cl^-(HCl)_m$ $[m,0]$[70a] and $Cl^-(H_2O)_n$ $[0,n]$,[70b] have of course been investigated previously, as well as neutral mixed species $(HCl)_n(H_2O)_n$, $n = 1, 2, 4$.[71] In order to understand the fragmentation and ligand exchange reactions observed in the mass spectrometer, we carried out quantum chemical calculations for both pure clusters, $[m,0]$ and $[0,n]$, and the mixed solvent clusters, $[m,n]$, with $m = 1-4$ and $n = 1, 2$. The most stable structures obtained in our calculations are shown in Figure 5, and their ligand binding energies, with a basis set superposition error (BSSE) of less

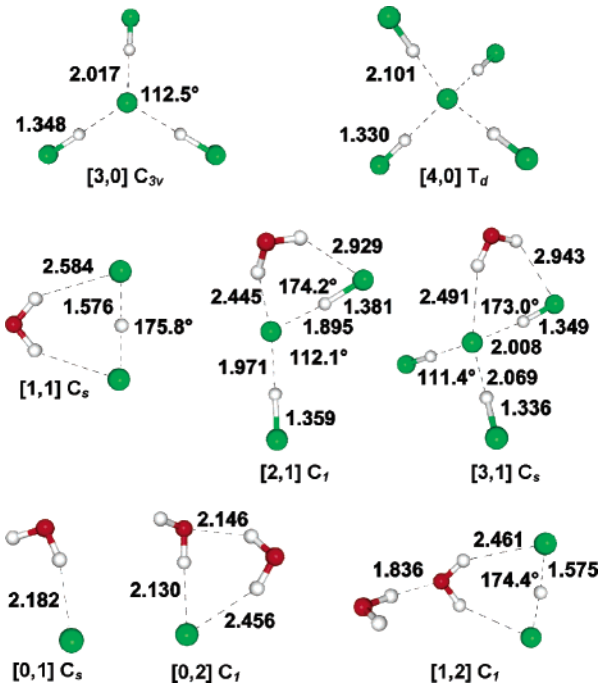

Figure 5. Calculated structures of mixed $Cl^-(HCl)_m(H_2O)_n$ listed in Table 1.

than 5 kJ/mol (<10%) on ΔE tested by the counterpoise method, are summarized in Table 1.

The simplest [1,0] compound is of course the well-known, linear centrosymmetric bichloride ion $[Cl-H-Cl]^-$, with one of the strongest known hydrogen bonds. Further coordination by molecular HCl results in very stable $Cl^-(HCl)_2$ = [2,0], $Cl^-(HCl)_3$ = [3,0], and even $Cl^-(HCl)_4$ = [4,0] ions. In general, our results are in good agreement with the previous MP2/6-311+G** studies, although there are some slight differences. While our DFT calculations predict a C_{3v} symmetry for [3,0] and a T_d symmetry for [4,0], the MP2/6-311+G** optimized structures yielded D_{3h} and distorted T_d symmetries, respectively, for [3,0] and [4,0].[70a]

The chloride anion forms stronger hydrogen bonds with HCl than with H_2O as clearly evidenced by the Cl^-...H distances. For instance, the hydrogen-bonding distances are 1.577 Å and 1.896 Å for [1,0] and, [2,0], respectively. The distances are much longer than 2 Å for both [0,1] and, [0,2], reflecting the disruptive effect of the ionic hydrogen bonds on the water network observed in infrared spectroscopy.[72-74] This can be understood, since the dipole moment of HCl always points along the direction of the hydrogen bond Cl^-...HCl resulting in maximum interaction. While HCl can of course form only a single hydrogen bond with Cl^-, H_2O can form two donor hydrogen bonds with the clusters. However, for example, in [1,1], [2,1], [3,1], and [1,2], a H_2O molecule bridges two Cl atoms via its O−H bonds, but the interaction is very weak with distances longer than 2.4 Å.

The relative strength of the hydrogen bonding of Cl^-...HCl and Cl^-...H_2O can also be seen by comparing the binding ener-

(70) (a) Chandler, W. D.; Johnson, K. E.; Fahlman, B. D.; Campbell, J. L. E. *Inorg. Chem.* **1997**, *36*, 776−781. (b) Xantheas, S. S. *J. Phys. Chem.* **1996**, *100*, 9703−9713.
(71) Chaban, G. M.; Gerber, R. B.; Janda, K. C. *J. Phys. Chem. A* **2001**, *105*, 8323−8332.
(72) Choi, J. H.; Kuwata, K. T.; Cao, Y. B.; Okumura, M. *J. Phys. Chem. A* **1998**, *102*, 503−507.
(73) Ayotte, P.; Weddle, G. H.; Johnson, M. A. *J. Chem. Phys.* **1999**, *110*, 7129−7132.
(74) Ayotte, P.; Weddle, G. H.; Kim, J.; Johnson, M. A. *J. Am. Chem. Soc.* **1998**, *120*, 12361−12362.

Table 1. Binding Energy (in kJ/mol), Including Zero-Point Corrected (ZPC) Energies, Thermal Enthalpies (ΔH), and Thermal Free Energies (ΔG) at Ambient Conditions, of a Ligand (HCl or H_2O) in $Cl^-(HCl)_m(H_2O)_n$ $[m,n]$[a]

			binding energy (kJ/mol), $[m,n] \rightarrow [m-1,n] + HCl$ or $[m,n] \rightarrow [m,n-1] + H_2O$						
			ΔE	ΔE_{BSSE}	$\Delta E_{+\Delta ZPC}$	$\Delta H_{298K,1atm}$		$\Delta G_{298K,1atm}$	
$Cl^-(HCl)_m(H_2O)_n$	$[m,n]$ and symmetry	ligand	calcd	calcd	calcd	calcd[b]	expt	calcd[b]	expt
Cl^-. . .(HCl)	[1,0] $D_{\infty h}$	−HCl	104.8	102.6	106.7	111.1 (103.4)	99.6 ± 8.4[c]	80.4 (72.5)	67[c]
Cl^-. . .$(HCl)_2$	[2,0] C_{2v}	−HCl	64.5	62.2	56.7	59.2 (57.5)	58.6[c]	31.3 (30.2)	33.1[c]
Cl^-. . .$(HCl)_3$	[3,0] C_{3v}	−HCl	53.0	50.6	47.3	48.0 (51.9)	49.0[d]	19.0 (21.4)	19.7[d]
Cl^-. . .$(HCl)_4$	[4,0] T_d	−HCl	43.7	40.8	38.6	38.9 (41.8)	43.1[d]	6.2 (21.2)	9.6[d]
Cl^-. . .(H_2O)	[0,1] C_s	$-H_2O$	62.1	60.8	57.2	60.5	61[f]	36.7	39[f]
Cl^-. . .$(H_2O)_2$	[0,2] C_1	$-H_2O$	60.5	57.4	49.9	53.0	53[f]	17.3	28[f]
Cl^-. . .$(HCl)(H_2O)$	[1,1] C_s	−HCl	90.7	87.7	90.1	93.2	66.9[e]	59.0	39.7[e]
Cl^-. . .$(HCl)_2(H_2O)$	[2,1] C_1	−HCl	56.5	54.2	48.7	49.5	51.5[e]	21.6	25.4[e]
Cl^-. . .$(HCl)_3(H_2O)$	[3,1] C_s	−HCl	47.3	44.5	42.0	42.4		11.3	
Cl^-. . .$(HCl)(H_2O)$	[1,1] C_s	$-H_2O$	48.0	45.9	40.6	42.7	43.9[e]	15.2	20.6[e]
Cl^-. . .$(HCl)_2(H_2O)$	[2,1] C_1	$-H_2O$	40.1	37.8	32.6	32.9	32[e]	5.5	13[e]
Cl^-. . .$(HCl)_3(H_2O)$	[3,1] C_s	$-H_2O$	34.4	31.8	27.3	27.3		0.1	
Cl^-. . .$(HCl)(H_2O)_2$	[1,2] C_1	−HCl	77.3	72.9	78.3	79.8	54.4[e]	50.6	27.3[e]
Cl^-. . .$(HCl)(H_2O)_2$	[1,2] C_1	$-H_2O$	47.0	42.7	38.0	39.7	40[e]	8.9	14.5[e]

[a] The energies are evaluated based on the optimized geometries for the most stable isomer at each cluster size n using the Gaussian 03 program at the B3LYP/6-311++G** level of theory. [b] The numbers in parentheses are the MP2/6-311+G** results from ref 70a. [c] Reference 75. [d] Reference 76. [e] Upschulte, B.L.; Evans, D.H.; Keesee, R.G.; Castleman, A.W. Unpublished results, referred to in ref 77. [f] Reference 78.

gies of the ligands, HCl and H_2O, for the various $[m,n]$ clusters, as summarized in Table 1. In most cases, the current DFT results agree with the experimental values within 4 kJ/mol, as well as with the previous ab initio calculations. The only exceptions are the $[1,n]$ clusters, in which DFT calculations seem to overestimate the HCl binding energies. However, in these cases the reliability of the experimental value cannot be determined, since the original data are unpublished. Interestingly, in those cases also the zero-point corrected binding energy is higher than the equilibrium energy, which is quite unusual. However, when the last HCl is lost, the frequency of the HCl vibration goes from around 800 cm^{-1} in the $(Cl-H-Cl)^-$ moiety of the cluster up to almost 3000 cm^{-1} in free HCl. This effect overcompensates the loss of vibrational degrees of freedom with a very low frequency.

Despite this uncertainty, as one could expect for all types of clusters the binding energies significantly decrease with their size. The strong hydrogen bonds between Cl^- and the HCl ligands found theoretically are in good agreement with our experimental observation, that, after a 40 s reaction delay, only the clusters of $[m,0]$ type with $m = 2-4$ remain in the ICR cell, Figure 4b. The ligand exchange reactions which contribute to their formation, $[m,n] + HCl \rightarrow [m+1,n-1] + H_2O$, are indeed calculated to be slightly exothermic, as summarized in Table 2. Such a ligand exchange reaction of [0,1] forming [1,0] was previously observed in a flow-tube reactor mass spectrometer.[79]

In order to gain more insight into the final stage of the fragmentation, calculations for various structures of the [4,6] cluster have been performed (Table 3 and Supporting Information). This particular cluster size was chosen because it is the largest cluster that is treatable with the computing resources available to us and gives an idea about the structural motifs operative in the larger, saturated species. Ab initio molecular dynamics simulations at 100 and 200 K were undertaken on low lying isomers, and the lowest-energy structure from these simulations was reoptimized at the B3LYP/6-311++G** level of theory. For these species, obviously six H_2O molecules are not sufficient to ionically dissolve four HCl molecules, and also in the larger saturated clusters it is to be expected that some HCl and H_2O coexist as covalent species in the cluster. Quite surprisingly, the lowest energy isomer of the [4,6] clusters consists of a distorted tetrahedral $Cl^-(HCl)_4$ unit, bound to a water hexamer in a modified book geometry.[80] Only slightly higher in energy is a similar structure with a planar water hexamer attached to a regular tetrahedron [4,6]a. Other isomers containing a water tetramer and a water dimer [4,6]b, or two water trimers [4,6]c, are also local minima on the overall potential surface, but they are considerably higher in energy Table 3. The isomer with all six water molecules evenly

Table 2. Energy (in kJ/mol), Including Zero-Point Corrected (ZPC) Energies, Thermal Enthalpies (ΔH), and Thermal Free Energies (ΔG) at Ambient Conditions, of Ligand Exchange[a]

		energy of ligand exchange (kJ/mol) $Cl^-(HCl)_m(H_2O)_n + HCl \rightarrow Cl^-(HCl)_{m+1}(H_2O)_{n-1} + H_2O$				
$Cl^-(HCl)_m(H_2O)_n$		$\Delta E_{+\Delta ZPC}$	$\Delta H_{298K,1atm}$		$\Delta G_{298K,1atm}$	
m	n	calcd	calcd	expt	calcd	expt
0	1	−49.5	−50.5	−23.0	−43.7	−19.1
1	1	−16.1	−16.6	−19.5	−16.1	−12.4
2	1	−14.8	−15.1		−13.6	
3	1	−11.3	−11.6		−6.1	
0	2		−40.2	−14.4	−41.7	−12.8

[a] The energies are calculated based on the binding energies listed in Table 1.

(75) Caldwell, G.; Kebarle, P. *Can. J. Chem.* **1985**, *63*, 1399−1406.
(76) Yamdagni, R.; Kebarle, P. *Can. J. Chem.* **1974**, *52*, 2449−2453.
(77) Keesee, R. G.; Castleman, A. W. *J. Phys. Chem. Ref. Data* **1986**, *15*, 1011−1071.
(78) Meot-Ner, M. M.; Lias, S. G. Binding Energies Between Ions and Molecules, and The Thermochemistry of Cluster Ions. In *NIST Chemistry WebBook, NIST Standard Reference Database Number 69*; Linstrom, P. J., Mallard, W. G., Eds.; National Institute of Standards and Technology: Gaithersburg MD, 20899, 2005.
(79) Amelynck, C.; Arijs, E.; Schoon, N.; Van, Bavel, A. R. *Int. J. Mass Spectrom.* **1998**, *181*, 113−121.
(80) Steinbach, C.; Andersson, P.; Melzer, M.; Kazimirski, J. K.; Buck, U.; Buch, V. *Phys. Chem. Chem. Phys.* **2004**, *6*, 3320−3324.

Table 3. Relative Energy and Evaporation Energy of a Ligand (HCl or H_2O) from [4,6] Including Zero-Point Corrected (ZPC) Energies, Thermal Enthalpies (ΔH), and Thermal Free Energies (ΔG) at Ambient Conditions, of the Isomers of [4,6][a]

	relative energy (kJ/mol)			
	ΔE	$\Delta E_{+\Delta ZPC}$	$\Delta H_{298K,1atm}$	$\Delta G_{298K,1atm}$
[4,6]	0.0	0.0	0.0	0.0
[4,6]a	13.5	8.5	11.3	0.1
[4,6]b	36.1	28.2	33.0	16.3
[4,6]c	73.0	58.2	67.8	42.2
[4,6]d	132.8	95.3	117.9	32.7

	evaporation energy (kJ/mol)			
	ΔE	$\Delta E_{+\Delta ZPC}$	$\Delta H_{298K,1atm}$	$\Delta G_{298K,1atm}$
$[4,6] \rightarrow [4,5] + H_2O$	51.9	38.4	42.8	−3.6
$[4,6] \rightarrow [3,6] + HCl$	35.0	30.7	30.4	4.3

[a] All energies (in kJ/mol) are relative to the isomer [4,6], the structure of which is shown in Figure 6 and the [4,6]a−d isomers are shown in the Supporting Information.

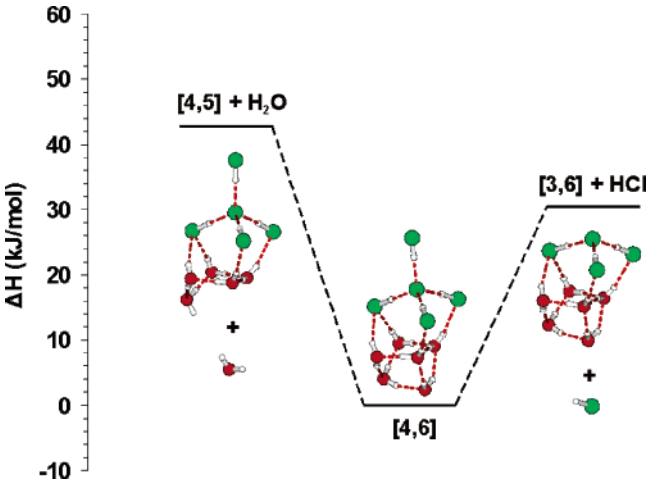

Figure 6. Potential energy surface for the elimination of HCl and H_2O from [4,6]. HCl loss is favored by 12.4 kJ/mol and is the only dissociation pathway observed in the experiment.

distributed over a T_d [4,0] ionic core [4,6]d is the least stable isomer. These results seem to be at odds with the ionic structure of $(HCl)_4(H_2O)_4$ found by Chaban et al.[71] However, the presence of Cl^- certainly has a dominant influence on the cluster structure. Moreover, Chaban et al. investigated only two isomers in which the heavy Cl and O atoms sit in the corners of a distorted cube, while phase-separated isomers have not been considered.

The calculated [4,6] structure suggests that we have observed a spontaneous phase separation in the gas phase. From a different point of view, one can see [4,6] as a self-assembled supramolecular structure of soft matter. Phase separation in the gas phase was recently observed for $Na(H_2O)_m(C_6F_6)_n^+$ by Patwari and Lisy via infrared photodissociation spectroscopy.[81] In the present case, it is quite intriguing that, in the presence of six water molecules, no HCl seems to be dissolved, although four water molecules are sufficient to dissolve one HCl in an overall neutral cluster.[82−89] The evaporation pattern in Figure 3 suggests that two to four additional H_2O molecules are required to stabilize an additional HCl for clusters larger than [4,6]. One may very well speculate that those additional HCl molecules are ionically dissolved in the cluster. In other words, a $Cl^-(HCl)_m(H_2O)_n$ cluster with $m > 4$ may consist of a tetrahedral $Cl^-(HCl)_4$ unit, while $(m - 4)$ HCl would be ionically dissolved.

The decay pathways of this species yields insight into the selective loss of H_2O vs HCl: experimentally, loss of HCl and formation of the [3,6] cluster is observed. The calculations for the most stable isomer [4,6] and its potential decay products [3,6] and [4,5] show that the enthalpy of $\Delta H_{vap} = 42.8$ kJ/mol for the loss of H_2O is 12.4 kJ/mol higher than that needed to evaporate HCl, $\Delta H_{vap} = 30.4$ kJ/mol (Figure 6). In the [4,6] cluster, each H_2O is bound via at least three hydrogen bonds, which makes loss of HCl preferred over H_2O.

Conclusions

Reactions of hydrated electron clusters $(H_2O)_n^-$, $n = 30-70$, with gaseous hydrogen chloride have been investigated using Fourier transform ion cyclotron resonance (FT−ICR) mass spectrometry. The proton, which is presumably formed by HCl dissolution, is reduced by the hydrated electron, with the weakly bound hydrogen atom evaporating from the cluster. The resulting $Cl^-(H_2O)_n$ clusters can then in subsequent collisions take up additional HCl molecules, a process in which three stages can be distinguished.

In the first stage, the clusters fragment, while additional HCl molecules are taken up by the clusters until they are saturated with HCl. In the second stage, the clusters lose ligands, both in collisions and by absorbing the ambient infrared radiation. At each point the ligand whose evaporation faces the smallest barrier, either HCl or H_2O, depending on the cluster composition, evaporates from the cluster, with clusters in specific size ranges containing specific numbers of dissolved HCl molecules. Finally, in the third stage the fragmentation of the smaller clusters slows down, and further reactions are dominated by ligand exchange of HCl for the remaining two to four water molecules, leaving eventually $Cl^-(HCl)_{2-4}$ clusters. The final product, the $Cl^-(HCl)_2$ cluster, is too tightly bound to fragment in ambient temperature collisions, so that its further fragmentation to the $D_{\infty h}$ proton bound bihalide anion $ClHCl^-$ is not observed.

The $Cl^-(HCl)_4(H_2O)_6$ cluster consists, according to the results of our calculations, of a distorted tetrahedral $Cl^-(HCl)_4$ unit and a booklike water hexamer connected to one side of the tetrahedron. The water hexamer is stabilized by a high number of hydrogen bonds, which makes loss of HCl preferential for this cluster size. Interestingly, this structure forms in the gas-phase in binary collisions with HCl and needs only the Cl^- anion as a structural anchor. Although four H_2O molecules are sufficient to dissolve one HCl molecule, no dissolution of HCl takes place in this cluster.

Acknowledgment. Financial support by the Deutsche Forschungsgemeinschaft, the Fonds der Chemischen Industrie, the

(81) Patwari, G. N.; Lisy, J. M. *J. Phys. Chem. A* **2003**, *107*, 9495−9498.
(82) Milet, A.; Struniewicz, C.; Moszynski, R.; Wormer, P. E. S. *J. Chem. Phys.* **2001**, *115*, 349−356.
(83) Bacelo, D. E.; Binning, R. C.; Ishikawa, Y. *J. Phys. Chem. A* **1999**, *103*, 4631−4640.
(84) Smith, A.; Vincent, M. A.; Hillier, I. H. *J. Phys. Chem. A* **1999**, *103*, 1132−1139.
(85) Re, S.; Osamura, Y.; Suzuki, Y.; Schaefer, H. F. *J. Chem. Phys.* **1998**, *109*, 973−977.
(86) Planas, M.; Lee, C.; Novoa, J. J. *J. Phys. Chem.* **1996**, *100*, 16495−16501.
(87) Lee, C. T.; Sosa, C.; Planas, M.; Novoa, J. J. *J. Chem. Phys.* **1996**, *104*, 7081−7085.
(88) Amirand, C.; Maillard, D. *J. Mol. Struct.* **1988**, *176*, 181−201.
(89) Ault, B. S.; Pimentel, G. C. *J. Phys. Chem.* **1973**, *77*, 57−61.

Alexander von Humboldt-Foundation (C.-K.S.), and the Heisenberg program of the Deutsche Forschungsgemeinschaft (M.K.B.) is gratefully acknowledged.

Supporting Information Available: Complete ref 46. Coordinates, harmonic frequencies and IR intensities, and thermochemistry of calculated structures shown in Figures 5 and 6, and isomers [4,6]a−d. Simulated IR spectra of structures shown in Figure 6 and isomers [4,6] a−d. This material is available free of charge via the Internet at http://pubs.acs.org.

JA067355O